2012 10th IAPR International Workshop on Document Analysis Systems

A Compact Size Feature Set for the Off-line Signature Verification Problem

Vu Nguyen
School of ICT
Griffith University
Gold Coast, Australia
vu.nguyen2@griffithuni.edu.au

Michael Blumenstein
SEET Group
Griffith University
Gold Coast Australia
m.blumenstein@griffith.edu.au

***Abstract*—With increasing computational power, researchers in the area of off-line signature verification have been able to investigate feature extraction techniques that produce large-dimensional feature vectors. However, a large feature vector is not necessarily associated with high performance. This paper investigates the performance of a small feature set consisting of 33 feature values. In the experiments using Support Vector Machines (SVMs), an average error rate (AER) of 16.80% was obtained together with a low false acceptance rate (FAR) for random forgeries of 0.19%. The significant reduction of the error rate was obtained when the proposed global features were employed, which demonstrates their astonishingly high discriminant power. These results suggest that the use of global features for the off-line signature verification problem is worth further investigation.**

***Keywords*-Off-line signature verification; Support Vector Machine; Variance feature; Energy feature; rotation invariant feature**

I. Introduction

Signature are a convenient form of biometric that have been legally accepted and widely used in society. This can be seen in the case of important government documents as well as day to day transactions using credit cards or personal cheques. Distinct from other biometrics, the collection and verification of signatures does not require special instruments. With the advent of computers and imaging capable gadgets, much effort has been put into the construction of reliable security systems based on the static image of signatures. Nevertheless, this problem remains unsolved despite decades of active research.

A crucial process often seen in signature verification systems is feature extraction. In this process, information that helps to distinguish the genuine signatures from the forgeries is extracted and retained. The technique employed in feature extraction can be categorized to be local or global based on the scope it uses to compute each component value. A component value of a local feature is computed using a small portion of the input pattern whilst the whole pattern must be inspected in order to compute any component value of a global feature. Compared to global features, local features tend to possess higher discriminating power due to the larger amount of information it captures from input patterns.

From the literature, it may be noted that researchers have employed local features favorably. Baltzakis and Papamarkos [1] used a feature set consisting of a 96-dimensional local feature and 16 global features. Justino *et al.* [2] employed a grid-based feature extraction scheme, which produces massive 2520-dimensional feature vectors. The feature values belong to four categories: Pixel Density, Gravity Center, Segment Curvature, and Predominant Slant. Variants of these features with other grid dimensions were also employed in the research of Swanepoel and Coetzer [3]. Ferrer *et al.* [4] used a 128-dimensional feature vector extracted from the polar and the Cartesian coordinates. Wen *et al.* [5] reported their best result was obtained using 144-dimensional rotation invariant Ring-Peripheral Features (RPF). Bertolini *et al.* [6] investigated combinations of 64 grid-based local features using a genetic algorithm. The dimension of the feature vectors employed in their research were ranging from 20 to 250.

Apart from the work of Baltzakis and Papamarkos, the reviewed literature indicates that global features did not attract much attention from researchers. Nevertheless, it is suggested that the discriminating power of a single global feature may be insignificant but the combination of multiple global features could produce a reverse effect. The present paper introduces a feature set consisting of a 24-D local feature and 4 global features. Despite the compact size of the 33-dimensional feature vector, encouraging results were obtained.

The remainder of this paper is organized as follows: The next section introduces the background and details of the proposed feature extraction techniques. After that, the experimental settings are described in Section III. It is followed by results and discussion in Section IV. Finally, Section V concludes and proposes directions for future research.

II. Feature Extraction

The feature set investigated in the present research consists of a local feature and four global features. The newly proposed global features are the Trajectory Length and Moment features. Both features are rotation invariant. The other two global features, Energy and Ratio features, were

978-0-7695-4661-2/12 $26.00 © 2012 IEEE
DOI 10.1109/DAS.2012.1

previously described in [7]. The following sub-sections describes the newly proposed feature extraction techniques.

A. Variance Feature

The mean and variance are important measures in probability and statistics. The variance describes how far numbers of a set are distributed from the mean value. It can be noted that in signature patterns, the mean and variance extracted from adjacent rows or columns are generally approximate. A sudden change in both mean and variance often indicates the existence of one or more strokes. It is proposed that an appropriate representation of these values could produce encouraging verification accuracies in signature verification.

Algorithm 1 Variance Feature Extraction

Require: Binary image $I(x, y)$
Require: Number of groups in the horizontal G_{hor} and vertical G_{ver} directions.
for $x = 1...width$ **do**
  $V_x^{col} \leftarrow var(y_i : I(x, y_i) = 1)$
  $M_x^{col} \leftarrow mean(y_i : I(x, y_i) = 1)$
end for
for $y = 1...height$ **do**
  $V_y^{row} \leftarrow var(x_i : I(x_i, y) = 1)$
  $M_y^{row} \leftarrow mean(x_i : I(x_i, y) = 1)$
end for
$size_{hor} \leftarrow width/G_{hor}$
$size_{ver} \leftarrow height/G_{ver}$
for $i = 1...G_{hor}$ **do**
  $f_i^{Hmean} \leftarrow \Sigma_{(i-1)*size_{hor}}^{i*size_{hor}} M_i^{col}$
  $f_i^{Hvar} \leftarrow \Sigma_{(i-1)*size_{hor}}^{i*size_{hor}} V_i^{col}$
end for
for $j = 1...G_{ver}$ **do**
  $f_j^{Vmean} \leftarrow \Sigma_{(j-1)*size_{ver}}^{j*size_{ver}} M_j^{col}$
  $f_j^{Vvar} \leftarrow \Sigma_{(j-1)*size_{ver}}^{j*size_{ver}} V_j^{col}$
end for
return $\{\{f_i^{Hmean}\}, \{f_i^{Hvar}\}, \{f_j^{Vmean}\}, \{f_j^{Vvar}\}\}$

To compute the Variance Feature, the mean and variance of the x and y coordinates of the black pixels are first computed for each row and column of the signature image. After that, the adjacent values of each type in either the horizontal or vertical direction are grouped together and the average values are calculated for each group. The final feature vector is created by rearranging the average values obtained in the previous step. The purpose of the averaging procedure is to create feature vectors with a predefined dimension. The whole process is presented in Algorithm 1.

B. Trajectory Length Feature

The first rotation invariant feature investigated in this research is Trajectory Length. This global feature utilizes information derived from the length of the pen movement/trajectory.

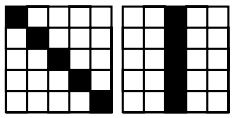
(a) (b)

Figure 1: Line segments having unequal length and area represented by the same number of pixels due to digitization

One notable characteristic of the length of the trajectory of a signature or handwriting is its invariability with respect to rotation. Moreover, the length of the pen's trajectory correlates with the total amount of energy consumed during the production of signatures, which is believed to be relatively stable between writing sessions for each individual. Although the length of the trajectory can be approximated with high precision directly from the trajectory of the pen, this information is not readily available in the static image of signatures. In the present work, the length of the trajectory is approximated by dividing the total length of all contours by 2. Another issue with the computation of the Trajectory Length feature is that line segments of different length can be represented by the same number of foreground pixels as a result of digitization. In order to obtain a more accurate approximation of trajectory length an adapted version of Harrington's curve length approximation algorithm [8] was employed.

The trajectory length feature described above was inspired by the Image Area feature employed by Papamarkos and Baltzakis in their signature verification research [9]. In that work, the Image Area feature was computed by simply counting the number of the foreground pixels of the skeleton representation of the signature. The advantages of the newly proposed trajectory length extraction technique over Papamarkos and Baltzakis's technique are both simplicity and accuracy. Skeletonization often requires more computation than contour extraction. The error rates produced by the counting technique employed by Papamarkos and Baltzakis for a single segment can be as high as 40%. This is illustrated in Fig. 1

C. Moment-based Feature

In the area of pattern recognition, researchers have investigated rotation invariant moments for many years. In his 1962 paper, Hu [10] described a set of 10 rotation invariant geometric moments up to the 3^{rd} order. However, high order moments introduce numerical instabilities and noise sensitivity, Kotoulas and Andreadis [11] commented. The following describes a feature based on Central moments.

From Hu's work, it can be seen that all the proposed rotation invariant moments utilizes the rotation invariant

property of the center ($\bar{x} = \frac{m_{10}}{m_{00}}, \bar{y} = \frac{m_{01}}{m_{00}}$) of the central moment

$$\mu_{pq} = \int_{-\infty}^{\infty}\int_{-\infty}^{\infty}(x-\bar{x})^p(y-\bar{y})^q\rho(x,y)d(x-\bar{x})(y-\bar{y}) \quad (1)$$

where m_{pq} denotes the (p+q)th order moment

$$m_{pq} = \int_{-\infty}^{\infty}\int_{-\infty}^{\infty}x^p y^q \rho(x,y)dxdy \quad (2)$$

and $\rho(x,y)$ is a continuous density function. For an image $I(x,y)$ of size $M \times N$, the (p+q)th moment is

$$\mu_{pq} = \Sigma_{-\infty}^{\infty}\Sigma_{-\infty}^{\infty}(x-\bar{x})^p(y-\bar{y})^q I(x,y) \quad (3)$$

Since the center is fixed in relation to any point of the set, the distance between any points and the geometric center does not change as the signature image rotates. In other words, these distances are rotation invariant. The following two feature values exploit that property:

$$f_1 = \Sigma_{x=0}^{M}\Sigma_{y=0}^{N}\sqrt{(x-x_0)^2+(y-y_0)^2}I(x,y), \quad (4)$$

$$f_2 = \Sigma_{x=0}^{M}\Sigma_{y=0}^{N}\frac{1}{\sqrt{(x-x_0)^2+(y-y_0)^2}}I(x,y) \quad (5)$$

The first feature value is the sum of the distances from every black pixel to the moment center and the second feature value is the sum of the inversions of those distances. These feature values are then divided by predefined constants to obtain values within the range 0..1. As the shape and size of genuine of signatures of an individual are relatively stable, its center of gravity and the above feature values can be considered stable as well and they can be used to distinguish genuine signatures from the forgeries.

D. The Camastra Feature

In the area of cursive handwritten character recognition, Thornton *et al.* [12] reported that the MDF was outperformed by the 34D feature set proposed by Camastra [13]. Camastra's feature set consists of a core 32D local feature and two global features aspect ratio ($\frac{width}{height}$) and the relative position of the baseline to the character itself. Having the number of feature values approximating the dimension of the proposed feature set, it is of interest to compare the performance of the Camastra feature with the proposed feature set.

In its recommended configuration for cursive character recognition, the input image is segmented using a 4×4 grid. The width and height of each grid cell are the rounded up value of corresponding dimensions divided by 4:

$$w = \left\lceil \frac{img_{width}}{4} \right\rceil \quad (6)$$

Table I: Experimental Settings

Phase	Genuine	Forgeries	
		Random	Targeted
Training	12	400	-
Testing	12	59	15

and

$$h = \left\lceil \frac{img_{height}}{4} \right\rceil \quad (7)$$

where $\lceil \cdot \rceil$ denotes the *ceiling* operator. Whilst the first three rows or columns of the grid are non-overlapping, the last two columns or rows of cells may be overlapped up to 3 pixels where the width or height is not divisible by 4. The impact of the overlap can be considered insignificant in images having large dimensions.

Once the grid lines have been determined, two distinct values are extracted from each grid cell. The first one is *density*, which is the proportion between the number of foreground pixels n_i in each cell and the area of a grid cell:

$$f_1 = \frac{n_i}{cell_{width} \times cell_{height}} \quad (8)$$

The other feature value is the difference between the sums of the second order of the number of pixels in the horizontal and vertical directions:

$$f_2 = \frac{1}{2}\left(1 + \frac{1}{hw^2}\Sigma_{i=1}^{h}n_i^2 - \frac{1}{h^2 w}\Sigma_{j=1}^{w}n_j^2\right) \quad (9)$$

where h and w are the width and height of each cell, respectively. In total, the core local feature consisted of $4 \times 4 \times 2 = 32$ elements.

Although the baseline feature had been integrated in the original work of Camastra, this information is not readily available in signatures. Consequently, Ratio feature was the only global feature employed along with the 32D local feature in the implementation of the Camastra feature in the present research. It should be kept in mind that the lack of the baseline feature may potentially be a factor that deteriorates the performance of the Camastra Feature in signature verification.

III. Experimental Settings

To facilitate the comparison of results, a subset of the publicly available GPDS-960 [14] signature database was employed in this research. The subset consists of the first 160 signature sets taken from the GPDS-960. Each set consisted of 24 genuine and 30 targeted forgeries. The signature images were in black and white with the resolution of 300dpi.

It is essential to employ a suitable number of genuine samples for the construction of signature models. Employing a large number of genuine signature may increase the

verification accuracy but the system will be less practical. Considering this trade-off between performance and robustness, only 12 genuine signatures were employed in the experiment with each signature set. Since the random forgeries can be collected more easily, the negative samples employed for training were generous with 400 genuine signatures randomly chosen from 100 other writers, four genuine signatures from each. In the testing process, the remaining 12 unused genuine signatures were employed. The forgeries for testing were 15 randomly selected forgeries of the signature set and 59 genuine signatures taken from the remaining 59 signature sets, one from each set. Table I summarizes the sample configuration for the training and testing phases. The experiment with each signature set was performed 30 times in order to obtain more stable results.

The construction of signature models in this research were performed using Support Vector Machines (SVMs) [15]. The choice of kernel for the SVMs varies depending on the classification problem and feature extraction techniques. Within the area of off-line signature verification, researchers often reported that their best results were obtained using the Radial Basis Function (RBF) kernel [4], [16]. Results from our previous investigation also concurs with this. Consequently, the RBF kernel was chosen. The experiments were conducted using SVM^{light} v6.01 software [17].

IV. Results and Discussion

Generally speaking, the detection of random forgeries are much easier compared to simulated or skilled forgeries. Many researchers have reported the false acceptance rate for random forgeries (FAR1) of less than 0.1%. The performance of their verification systems are often reported using the lowest average error rate (AER) obtained which is the average value of the false rejection rate (FRR) of genuine signatures and the false acceptance rate for simulated forgeries (FAR2): AER $= \frac{\text{FRR}+\text{FAR2}}{2}$. In the present research, the experimental results are reported using these measurements.

Table II: Experimental Results of the Variance feature

σ	FRR	FAR1	FAR2	AER
4.0	20.15%	1.01%	25.08%	22.61%
6.0	21.49%	0.86%	23.17%	22.33%
8.0	**23.03%**	**0.75%**	**21.37%**	**22.20%**
10.0	24.80%	0.65%	19.76%	22.28%

Table II presents the experimental results of the Variance feature. It can be seen that the performance of the Variance feature, being used individually, is relatively low with the AER being as high as 22.20%. However, these results were not unexpected as the Variance feature is fairly simple with only 24 feature values.

As can be seen from Table III, the best AER of the Camastra feature set without the baseline feature was 20.33%. This result is nearly 2% better than the Variance feature due to the larger 33-D feature vector of the Camastra feature compared to the 24-D feature vector of the Variance feature.

Table III: Experimental Results of the Camatra feature

σ	FRR	FAR1	FAR2	AER
0.3	16.73%	1.25%	29.7%	23.22%
4	12.92%	0.94%	31.23%	22.08%
40	19.89%	0.23%	20.77%	**20.33%**
45	21.4%	0.2%	19.32%	20.36%

Table IV: Experimental Results of the Variance feature in conjunction with the Global Features

σ	FRR	FAR1	FAR2	AER
7.0	13.43%	0.22%	20.48%	16.955%
8.0	**15.16%**	**0.19%**	**18.43%**	**16.80%**
9.0	17.23%	0.15%	16.66%	16.945%
10.0	19.18%	0.13%	14.98%	17.08%

When other global features were employed as compliments to the Variance feature, the verification accuracy was improved significantly. The new AER obtained was 16.80%, which is a 5.4% improvement from the earlier 22.20% AER. The corresponding false acceptance rate for random forgeries (FAR1) at that operational point was also reduced significantly, from 0.75% down to 0.19%. Table IV details the results of this experiment. These figures compare favorably to the results obtained using the MDF-based feature sets previously reported in [7]. More importantly, the total number of feature values of the newly proposed feature set is only 33 compared to the dimension of more than 120 of the MDF-based feature set. This AER of the proposed feature set is also 3.53% better than the best result of the Camastra feature.

Table V: Experimental Results of the Camastra feature in conjunction with the Global Features

σ	FRR	FAR1	FAR2	AER
22	14.75%	0.12%	18.02%	16.385%
24	16.22%	0.11%	16.59%	16.405%
26	17.61%	0.09%	15.15%	**16.38%**
28	19.15%	0.08%	13.85%	16.5%

The proposed set of global features can also be used to reduce the error rates of the Camastra feature. A significant improvement of nearly 4% was observed when the global features were combined with the Camastra feature. The results of this experiment are presented in Table V.

Table VI and Fig. 2 conclude this section by summarizing the dimension and the AER and depicting the ROC curves of the feature sets investigated in this research.

V. Conclusions and Future Work

Local feature extraction techniques have been investigated intensively in the area of off-line signature verification. In many cases, the dimensions of the feature vectors are large,

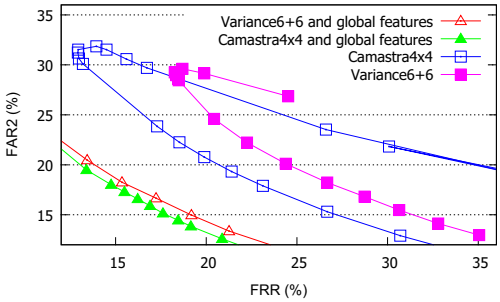

Figure 2: The ROC curves of the feature sets as functions of σ of the RBF kernel of the SVMs

Table VI: The performance comparison of the feature sets

Feature Set	Size	AER
MDF-based [7]	128	17.25%
Camastra + Global features	42	**16.38%**
Camastra	33	20.33%
Variance + Global features	33	16.80%
Variance	**24**	22.20%

ranging from hundreds to thousands. Large size features tend to create a heavy load on the classifiers employed. In addition, they can diminish the impact of "good" but small sized add-on features. Nevertheless, the present research has demonstrated that competitive results could be obtained using relatively small dimensional feature set by employing global features. Under the specific experimental settings described, the proposed feature set compares favorably to the MDF and Camastra features in terms of both discriminating power as well as feature vector size.

Despite the encouraging results, there are significant gaps between the performance of the proposed feature set and other state-of-the-art local feature extraction techniques. However, it is strongly believed that these performance gaps could be bridged by employing more global features. Future investigations will focus on other moment-based rotation invariant features and the fusion of global features.

ACKNOWLEDGMENT

The experiments reported in this research were conducted using the Griffith University HPC Cluster - V20z.

REFERENCES

[1] H. Baltzakis and N. Papamarkos, "A new signature verification technique based on a two-stage neural network classifier," *Engineering Applications of Artificial Intelligence*, vol. 14, no. 1, pp. 95–103, 2001.

[2] E. J. R. Justino, F. Bortolozzi, and R. Sabourin, "A comparison of SVM and HMM classifiers in the off-line signature verification," *Pattern Recognition Letters*, vol. 26, no. 9, pp. 1377–1385, 2005.

[3] J. P. Swanepoel and J. Coetzer, "Off-line signature verification using flexible grid features and classifier fusion," in 12^{th} *ICFHR*, 2010, pp. 297–302.

[4] M. A. Ferrer, J. B. Alonso, and C. M. Travieso, "Offline geometric parameters for automatic signature verification using fixed-point arithmetic," *IEEE PAMI, Trans. on*, vol. 27, pp. 993–997, 2005.

[5] J. Wen, B. Fang, Y. Y. Tang, and T. Zhang, "Model-based signature verification with rotation invariant features," *Pattern Recognition*, vol. 42, no. 7, pp. 1458–1466, 2009.

[6] D. Bertolini, L. S. Oliveira, E. J. R. Justino, and R. Sabourin, "Reducing forgeries in writer-independent off-line signature verification through ensemble of classifiers," *Pattern Recognition*, vol. 43, no. 1, pp. 387–396, 2010.

[7] V. Nguyen, M. Blumenstein, and G. Leedham, "Global features for the off-line signature verification problem," in 10^{th} *ICDAR*. IEEE Computer Society, 2009, pp. 1300–1304.

[8] S. J. Harrington, "Determination of the arc length of a curve," U.S. Patent 5 317 650, 5 31, 1994.

[9] N. Papamarkos and H. Baltzakis, "Off-line signature verification using multiple neural network classification structures," in 13^{th} *ICDSP*, vol. 2, 1997, pp. 727–730 vol.2.

[10] M.-K. Hu, "Visual pattern recognition by moment invariants," *IRE Transactions on Information Theory*, vol. 8, pp. 179–187, 1962.

[11] L. Kotoulas and I. Andreadis, "Image analysis using moments," in 5^{th} *ICTA*, 2005.

[12] J. Thornton, J. Faichney, M. Blumenstein, V. Nguyen, and T. Hine, "Offline cursive character recognition: A state-of-the-art comparison," in 19^{th} *IGS*, 2009.

[13] F. Camastra, "A SVM-based cursive character recognizer," *Pattern Recognition*, vol. 40, pp. 3721–3727, 2007.

[14] F. Vargas, M. Ferrer, C. Travieso, and Alonso, "Offline handwritten signature GPDS-960 corpus," in 9^{th} *ICDAR*, Paranã, Brazil, 2007.

[15] V. Vapnik, *Statistical Learning Theory*. New York: Wiley, 1998.

[16] H. Lv, W. Wang, C. Wang, and Q. Zhuo, "Off-line Chinese signature verification based on support vector machines," *Pattern Recognition Letters*, vol. 26, no. 15, pp. 2390–2399, 2005.

[17] T. Joachims, "Optimizing search engines using clickthrough data," in *KDD*. ACM, 2002, pp. 133–142.